1

Orogenesis and Climate

Frédéric FLUTEAU[1], Delphine TARDIF[2,3], Anta-Clarisse SARR[4], Guillaume LE HIR[1] and Yannick DONNADIEU[4]

[1] *Institut de physique du globe de Paris, Paris Cité University, France*
[2] *LSCE, Gif-sur-Yvette, France*
[3] *Institut de Recherche pour le Développement, Montpellier, France*
[4] *CEREGE, Aix-en-Provence, France*

1.1. Introduction

Climate is controlled by the incoming solar energy (a quantity that depends on the latitude of the site, the solar constant and the obliquity and climatic precession), the greenhouse effect related to the atmospheric composition and the energy redistribution by atmospheric and oceanic circulation. Climate also depends on the exchanges (energy, matter and momentum) between the components of the climate system: atmosphere, ocean, cryosphere, biosphere, lithospheric surface. A disturbance applied to one or more of these components leads to a destabilization of the system, resulting in climate change. Climate changes have various causes and occur at all timescales. Causes can be internal to the climate system and related to the natural variability of physical processes, such as the ocean–atmosphere coupling or the instability of an ice cap, as well as external to the climate system, such as plate tectonics and one of its features, orogeny.

Himalaya, Dynamics of a Giant 3,
coordinated by Rodolphe CATTIN and Jean-Luc EPARD.

In this chapter, we discuss how orogenesis alters the climate system. To do so, we take the example of the uplift of the Himalayan range and Tibetan plateau, as a result of the India–Asia collision (see Volume 1 – Chapter 1). After a short description of the present-day climate in Asia, we describe the climate evolution during the Cenozoic at the global scale and in Asia. We use climate modeling studies to understand the responses of the atmosphere and the ocean to mountain uplift. A climate model is a mathematical representation of the climate system. It simulates the climate at equilibrium with imposed boundary conditions such as paleogeography, atmospheric chemistry, and Earth's orbital parameters. Modifying the boundary conditions thus allows us to quantify the impact of these factors on the climate.

The climatic impact of an orogeny is not limited to the response of the atmospheric and oceanic circulation, but also induces an indirect response of the climate system by affecting the carbon cycle. Indeed, changes in temperature and precipitation that may occur as a result of orogeny will in turn affect the physical erosion of landforms (see Volume 3 – Chapter 2). Additionally, sediments can undergo chemical erosion that will further disrupt the carbon cycle and therefore the climate. Other mechanisms are also likely to act on the carbon cycle, such as the burial of organic matter. This orogeny–carbon cycle–climate relationship has been studied in the case of the Himalayan orogeny.

1.2. Climate in Asia: present and past

1.2.1. *Present-day climate*

Asia has an extremely contrasted climate. A large southern and southeastern area, stretching from Pakistan to eastern China, undergoes the seasonal reversal of monsoon flow (South Asian monsoon from Pakistan to Myanmar and East Asian monsoon from Myanmar to eastern China). A vast region to the west and north of the Tibetan plateau (from Iran to Mongolia) experiences a semi-arid to arid climate, while further north, Siberia is dominated by a continental to polar climate. This dichotomy between the warm and seasonally wet climates of south and eastern Asia and the inland arid belt is due to the presence of high mountain ranges (Himalaya, Karakorum, Pamir, Hindu Kush, Zagros) and the Tibetan plateau, which strongly limits the atmospheric exchanges between the low and mid-latitudes of Eurasia. The Asian monsoon is marked by a strong seasonality of precipitation (with most precipitation occurring during summer), coupled with a reversal of the atmospheric circulation. Halley (1686) described the monsoon as a result of differential heating between the Indian Ocean and the Asian continent. This approach is still widely used (Webster et al. 1998), even though some scientists consider monsoon as the manifestation of the seasonal migration of the intertropical convergence zone.

In winter, in the mid-latitudes of Asia (mostly Siberia), the low insolation and the continentality amplified by the snow albedo-temperature feedback cause extremely low temperatures and generate the Siberian anticyclone, the densest air masses in the Northern Hemisphere, which is maintained by radiative cooling at the surface and large-scale descending motion (Ding and Krishnamurti 1987). A strong temperature gradient between the cold Asian continent and the mild Pacific Ocean results in the advection of cold and dry continental air to the northeastern China. To the south, East Asian winter monsoon generates moderate precipitation over the southeastern China (Figure 1.1) fed by moist air blowing from the nearby Pacific ocean (Figure 1.2).

At the end of the winter season, the increase in insolation over the northern hemisphere favors the rise of surface temperatures, which are also amplified locally by the decrease of albedo due to the melting of snow cover. Over southern Asia, convective systems develop and a low-pressure cell settles over India. At the end of spring, surface heating of a large part of Asia continent leads to the establishment of deep convection. In summer, the peak upper-tropospheric temperatures at 300 hPa (about 9,500 m high) located to the south of the Tibetan plateau are thermodynamically coupled to the precipitating convection (Boos and Kuang 2010). At the surface, a deep low-pressure cell stretches over southern Asia up to the Arabian Peninsula and conveys air masses from the Indian Ocean (Figure 1.2). Despite a moderate mean elevation of about 2,000 m, except in the Ethiopian region, the East African highlands constitute an orographic barrier for the air masses advected by the Indian low pressure. The low-level cross-equatorial flow, referred to as the Somali jet, carries moisture that leads to heavy precipitation over Asia. While reaching India, the humid air mass hits the Great Escarpment of the Deccan Traps, a pile of basaltic lava flows culminating at 1,700 m in the Western Ghats, leading to strong precipitation on the coastal fringe (Figure 1.1), causing recurrent catastrophic floods in the metropolis of Mumbai and its 20 million inhabitants. To the east of the Ghats landform, rainfall is less

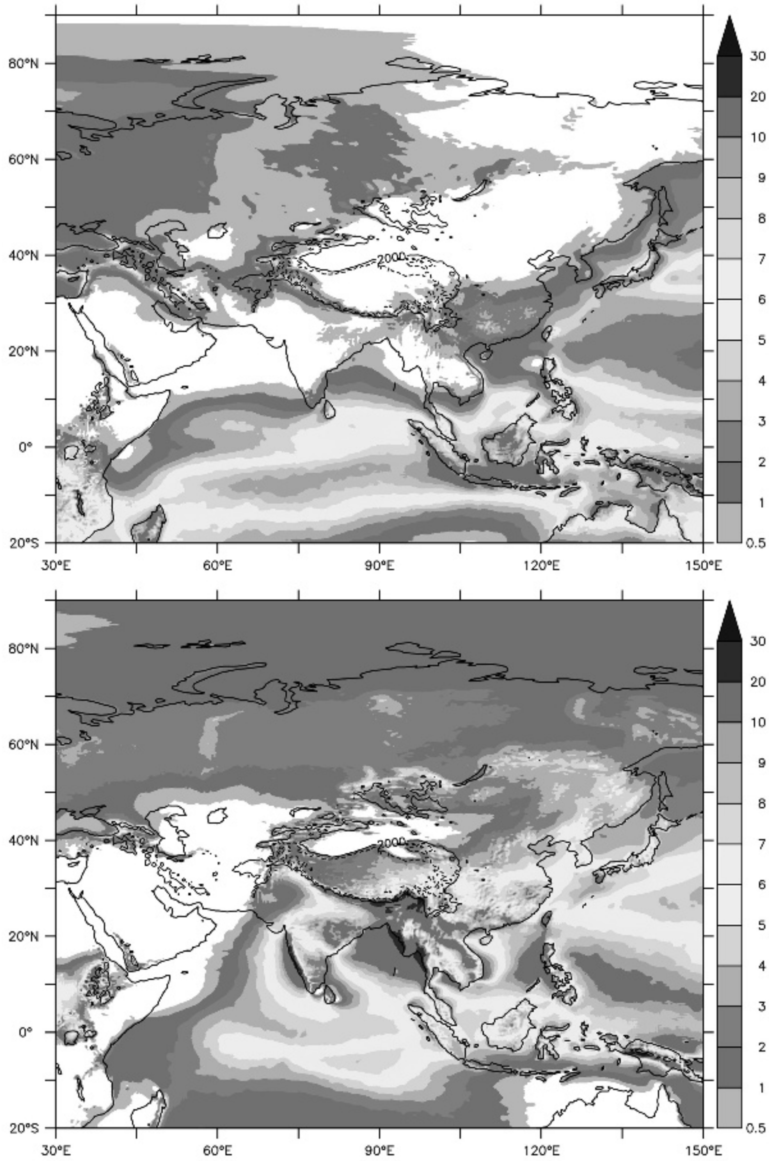

Figure 1.1. *Mean precipitation in winter (top) and summer (bottom) (in mm/day) (data are from ERA5 reanalysis (Hersbach et al. 2019)). Topography contoured at 2,000 m (4,000 m) in a thin solid (dash) line. For a color version of this figure, see www.iste.co.uk/cattin/himalaya3.zip*

intense due to a rain shadow effect. The air masses are reloaded with moisture over the Bay of Bengal, before hitting the Indo-Burmese range to the east and the Himalayan range to the north (Figure 1.2), causing an intense orographic rainfall (Figure 1.1). Indeed, the Himalaya forms an east–west gigantic barrier to the north of the alluvial plains of the Indian subcontinent. As the air masses are lifted on the lee of the Himalaya and in the convective systems, they cool down, thus decreasing the maximum water vapor they can contain, according to the Clausius–Clapeyron relationship. When the saturation vapor pressure is reached, the water vapor condenses on nuclei (mineral dust, salt crystal, volcanic ash) to form water droplets (or ice crystals depending on the air temperature), leading to cloud formation. Water condensation released a large amount of latent heat which self-sustains the monsoon circulation in Asia. Water droplets grow by coalescence in the clouds and turn to heavy rainfalls. The eastern part of the Tibetan plateau also experiences strong summer precipitation, while the western part of the plateau is drier (Figure 1.1).

We will now propose an overview of how the climate has evolved since the India–Asia collision based on paleoclimatic indicators.

1.2.2. *Cenozoic climate evolution*

The Earth's climate during the Cenozoic is marked by a succession of slow changes interspersed with abrupt transitions. After the Early Eocene climatic optimum (~50 Ma), during which the Earth experienced a globally hot climate, a slow cooling is recorded, ending with the formation of the Antarctica ice cap around the Eocene–Oligocene boundary (~34 Ma) (Ladant et al. 2014; Westerhold et al. 2020). This unipolar glaciation persisted through the Oligocene and Early Miocene. The Earth undergoes a new cooling period starting at ~14 Ma, which lead to the final build-up of the Antarctic ice sheet approximately 13–14 Ma followed by the Greenland glaciation at the end of the Miocene (~6 Ma).

Asia has undergone important climatic changes during the Cenozoic that can be deduced from different proxies (lithology, flora, isotopes, etc.). These evidences are numerous and we will focus on a few sites only. During the early Cenozoic (Paleocene–Eocene) at the time of the India–Asia collision, southern Asia experienced a warm and wet climate as evidenced by the fossil flora discovered in western India (Rajasthan, Gujarat) (Spicer et al. 2017; Bathia et al. 2021).

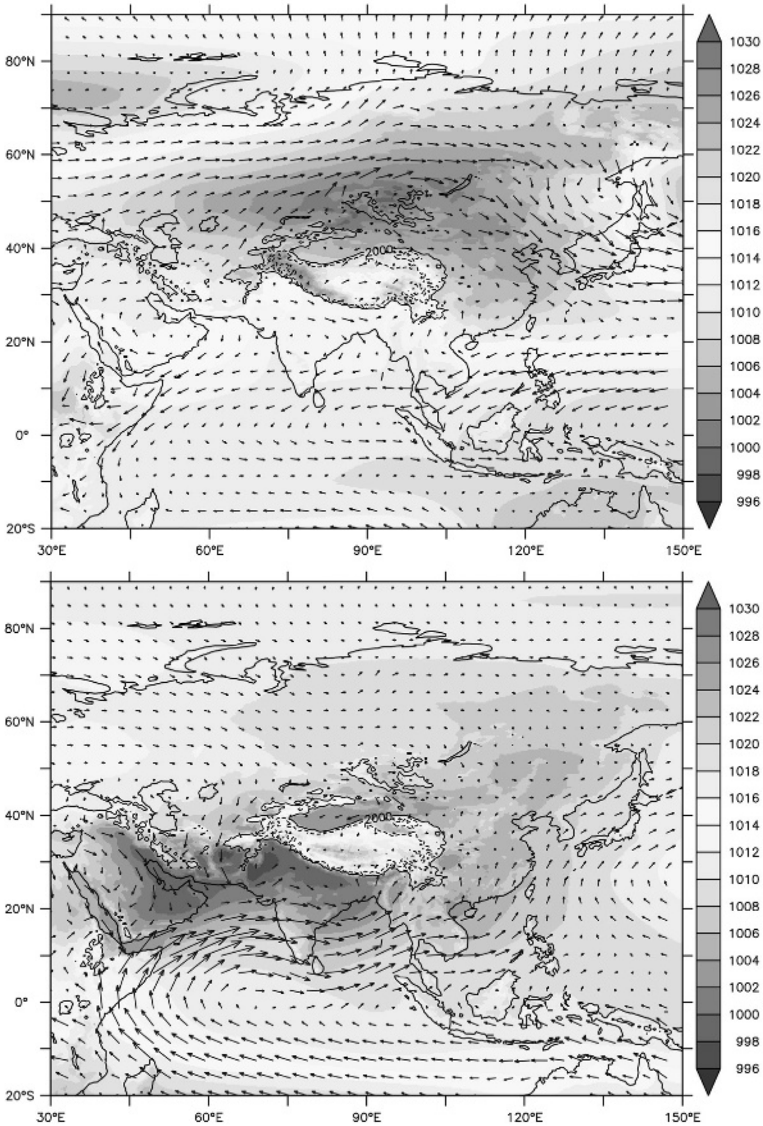

Figure 1.2. *Mean sea level pressure (shading – in hPa) and 850 hPa wind (vector) in winter (top) and summer (bottom) (data are from ERA5 reanalysis (Hersbach et al. 2019)). Light to dark blue colors are for low pressure, yellow to orange colors are for high pressure. Topography contoured at 2,000 m (4,000 m) in a thin solid (dash) line. For a color version of this figure, see www.iste.co.uk/cattin/himalaya3.zip*

In Burma, low oxygen isotope values (δ^{18}O) of freshwater gastropod shells from the Late Eocene indicate a marked seasonality of precipitation (Licht et al. 2014). Farther east, in the Yunnan Basin (China), xerophytic flora and sedimentation consisting of red sandstone and gypsum provide evidence of a warm and semi-arid climate that persisted until the early Late Eocene (~41 Ma) (Fang et al. 2021) followed by a warm and wet climate in the late Eocene (~35 Ma) (Sorrel et al. 2017). In central Tibet, an abundant fossil flora from the middle Eocene (~47 Ma) found in the Bangor Basin reflects a subtropical climate and seasonal rainfall (Su et al. 2020). This floristic assemblage has strong affinities with European and North American flora but very little with Gondwanan flora of India, suggesting the presence of high landform in the south of this basin (Gangdese Uplands) prior to the rise of the Himalaya. All of these sites, except the Yunnan site, record more or less pronounced seasonality of precipitation that has been interpreted as evidence of a monsoonal regime as early as the Eocene (Licht et al. 2014) or the seasonal migration of the intertropical convergence zone (Bathia et al. 2021).

The onset of a modern monsoon regime in Asia is thought to date from the early Miocene based on paleobotanical and lithological data (Sun and Wang 2005). This is coeval with the intensification of chemical weathering of the sediment deposited on the continental margin of the South China sea, as recorded by the K/Al ratio (Clift and Webb 2019). The appearance of upwelling-sensitive planktic foraminifer Globigerina bulloides off the Oman margin driven by the summer monsoon wind is much more recent, ~13 Ma (Gupta et al. 2015). Thus, the age of onset of the modern monsoon regime has long been debated. We will see that this paradox is now resolved (Sarr et al. 2022). During the late Miocene, the intensity of the Asian monsoon decreases in response to global cooling. Oxygen isotope analysis on fossil freshwater bivalve shells and mammal teeth from the Himalayan foreland yields the seasonal δ^{18}O variation in surface waters that suggests a decline in precipitation approximately 7.5 Ma (Dettman et al. 2001). This agrees well with a diachronous change in vegetation from trees and shrubs (using the C3 photosynthetic pathway) to grassland (using the C4 photosynthetic pathway) found in the Siwaliks in the Himalayan foothill (Quade et al. 1989; Tauxe and Feakins 2020) and ranging from 7.8 Ma in Pakistan to 6 Ma in Nepal, together with the evidence of grassland expansion recorded in the Weihe Basin (central China) (Zhao et al. 2020).

In Central Asia, the climatic evolution is very different. The Asian continental interior becomes more arid from the Late Eocene onward. Eolian sedimentation associated with gypsum deposited in the Xining Basin is representative of playa-lake environment (Meijer et al. 2019) in which a xerophytic fossil flora develops (Barbolini et al. 2020). This trend is reinforced from the Oligocene onward with the gradual disappearance of gypsum in the Xining Basin (Fang et al. 2015). Loess deposits in northwest China dated to the Lower Miocene (~22 Ma) are interpreted as a marker of the winter monsoon (Guo et al. 2008). An arid climate has persisted since the early Miocene (Barbolini et al. 2020).

To understand the climatic impact of paleogeographic changes, climate modeling proves to be a relevant tool. However, this requires first reconstructing the paleo-elevation of landforms.

1.3. Reconstructing the paleo-elevation of landforms

Orogenesis leaves structural and petrological markers that can be used to identify past deformation. However, the main difficulty lies in estimating the paleo-elevation of the landforms. We discuss hereafter the three main methods employed to obtain paleo-elevation estimates.

The relationship linking leaf physiognomy (size, shape, thickness, type of leaf margin) to climate is assumed to have remained constant over time. The analysis of specific morphological features of the fossil leaves therefore makes it possible to estimate the paleo-temperature at one site. Moreover, by comparing the fossil flora to a nearby site of similar age known to be located at sea level, we can deduce the paleo-elevation of the site by fixing the lapse rate (which varies from 4°C/km to 10°C/km) or enthalpy (Spicer et al. 2018). This method is calibrated on dicots and does not take into account all biogeographic regions (such as Australia) or taxa (such as conifers). It cannot be employed before the upper Cretaceous since the flowering plants appear during the Cretaceous.

A second method is based on the oxygen isotope measurement in pedogenic and lacustrine carbonates (Rowley and Garzione 2007). The ratio of heavy to light oxygen isotopes, when compared to a global reference value (namely the Vienna standard mean ocean water, VSMOW), is noted (δ^{18}O). The decrease of δ^{18}O with altitude reflects a depletion in heavy isotope (^{18}O) of precipitation along the trajectory of the air mass (Rayleigh-type distillation process) (Mulch et al. 2016). Assuming the precipitation-calcite thermodynamic equilibrium, the $\delta^{18}O$ of lacustrine and pedogenic carbonates represents the isotopic signature of rainfalls and thus the paleoaltitude of the site. This tool has, however, some drawbacks: 1) the isotopic data represents surface water catched by the draining basin rather than rainfall and 2) the isotopic signature depends on the air mass pathway. To circumvent this difficulty, a new promising tool referred to as the clumped isotope measurement Δ_{47} has been developed. The clumped isotope measurement relies on the propensity to form molecules containing bonds between heavy isotopes of carbon and of oxygen in a carbonate. The quantity of bonds is a function of the temperature.

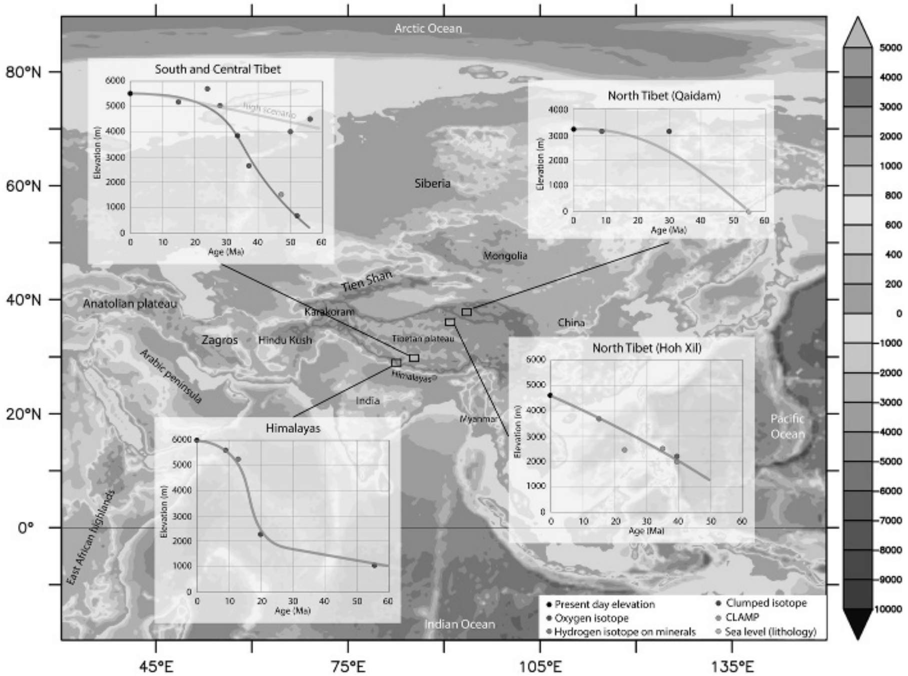

Figure 1.3. *Shading: present-day geography (m). Plots display the paleo-elevation of the Himalaya, Southern and Central Tibet, Hoh Xil basin and Qaidam basins. The filled circles represent different proxies of paleo-elevation. The gray curves are indicative of the elevation during the Cenozoic. For a color version of this figure, see www.iste.co.uk/cattin/himalaya3.zip*

These tools have been employed to reconstruct the paleo-elevation of landforms in Asia (Figure 1.3). The southern and central Tibetan Plateau are thought to have reached a high elevation of ~4 km by the late Eocene (Ding et al. 2017). This scenario, however, remains debated because the $\delta^{18}O$ of rainfall could be biased by climatic processes. Indeed, an increase in convective precipitation or a different air mass trajectory may result in a decrease of δ^{18}O of rainfall, suggesting a relief higher than it actually was (Botsyun et al. 2019). The Himalayan range reaches its current elevation in the middle Miocene ∼15 Ma (Gébelin et al. 2013; Ding et al. 2017). The northern part of Tibet and the ranges north of the Tibetan Plateau (Tien Shan, Altai) mostly rise from the Miocene onward.

1.4. The contribution of climate modeling

The understanding of the effects of landforms on the atmospheric circulation began with the pioneering work of Charney and Eliassen (1949) on the disturbances induced by mountain ranges on the mid-latitude jet stream. Bolin (1950) clarified the landform–atmosphere relationship by studying the influence of Asian and North American landforms on the mid-latitude westerlies, temperature and surface pressure. The turn of the 1960s marks the development of the first climate model that is a mathematical representation of the processes governing the climate system. The first models, also called general circulation models, only simulated the atmosphere circulation. Yet, in the mid-1960s, Mintz (1965) already showed that the Tibetan plateau plays a determining role in the development and location of the Siberian anticyclone. Since the 1970s, atmospheric general circulation models include an explicit representation of the hydrological cycle and clouds. The other components of the climate system (ocean surface temperature, sea ice extent, etc.) are considered as prescribed boundary conditions. Nevertheless, several important results were obtained: the uplift of landforms (Tibet, Rocky Mountains) controlled the distribution of precipitation (Manabe and Terpstra 1974), favoring the drying of the continental interior and intensifying the summer monsoon in Asia (Hahn and Manabe 1975). In the late 1980s, Kutzbach et al. (1989) showed how the mid-latitude upper-tropospheric planetary waves increase with mountain uplift and how low-tropospheric winds are diverted by topography. They emphasized the consistency of the simulated climate changes due to uplifts with late Cenozoic climate indicators (Ruddiman and Kutzbach 1989). Until the early 1990s, studies were conducted by modifying the height of the landform on a present-day geography. Subsequent work considers late Cenozoic paleogeographic changes to assess the impact of landform changes (Fluteau et al. 1999).

More sophisticated climate models referred to as Earth system models were developed in the early 2000s and have benefited from the development of high-performance computing. These climate models simulate the atmosphere, the ocean, the sea ice, the land surface and vegetation and the biogeochemistry of the ocean. The atmospheric and oceanic components are described by a set of equations representing dynamic processes (differential equations of fluid motion calculated on a 3D grid) and physical processes (calculated on a single atmospheric column such as radiative balance, clouds, precipitation, exchanges with other components of the climate system). The land surface model simulates the vegetation, soil and water routing (McGuffie and Henderson 2005; Sepulchre et al. 2020). Because of their very long response time ($>10^3$ years), ice-sheets are prescribed in the same way as paleogeography, solar constant, atmospheric chemistry and Earth's orbital parameters. Sensitivity experiments to paleogeographical changes allow us to simulate the consequences of uplift on each component of the climate system. Finally, model-data comparison remains an essential step to test the validity of these scenarios.

1.4.1. *Impact of orogenesis on the atmospheric circulation*

The strengthening of the summer monsoon in Asia has regularly been attributed to the uplift of the Tibetan plateau alone, as the heating of its surface favors the convergence of air masses (Kutzbach et al. 1989). However, these early studies did not separate the uplift of the Tibetan plateau from that of the Himalaya. In fact, it has been shown that the South Asian summer monsoon is little impacted when the Tibetan plateau is suppressed and the Himalaya kept at their current elevation (Boos and Kuang 2010; Acosta and Huber 2020). Indeed, a deep convection is set up over northern India leading to the development of a low-pressure area over the Gangetic plain driving the advection of moist air masses from the Indian Ocean. Arriving on the Himalaya, moisture flux condenses and produces orographic precipitation. Maffre et al. (2018) showed that the monsoon in Asia weakens considerably when global landforms are lowered down to 200 m. The low pressure located over northern India and responsible for the advection of moist air mass from the Indian Ocean is replaced by a huge low-pressure area centered in Mongolia stretching over a large part of Eurasia. It results in a decrease of 60–80% of precipitation in the South Asian monsoon domain.

The uplift of Tibet also acts on the circulation of air masses at mid-latitudes, and in particular on the location of the jet stream. With a high Tibetan plateau (>3,000 m), Zoura et al. (2019) shows that the jet stream migrates further north in summer, which increases precipitation in spring (pre-monsoon) and summer (monsoon) in eastern China. Central Asia experiences an aridification when the Tibetan plateau and adjacent landforms are uplifted, which largely explains the observed climatic evolution in this region since the Eocene.

Most of the early work to understand the interaction between topography and the atmospheric circulation was based on sensitivity experiments to the landforms (Tibet, Himalaya) in a modern geographical context. To understand the evolution of the Cenozoic climate, all paleogeographic changes (continental drift, evolution of oceanic basins and epicontinental seas as well as evolution of all landforms) must be taken into account. Tardif et al. (2020) recently showed that in the Late Eocene, the monsoon regime over southern Asia is driven by the seasonal migration of the intertropical convergence zone (Figure 1.4).

The paleogeography at that time is very different from that of the present day with lower landforms, a huge epicontinental sea in Eurasia – the Paratethys – and a largely flooded Arabian Peninsula.

The simulated climate is generally in good agreement with the data except for the Tibetan plateau which is too arid. The onset of a monsoon regime similar to the present-day one in Asia occurs in experiment with the Early Miocene boundary conditions in response to the important paleogeographic changes in Asia (uplift of the Himalaya and adjacent landforms and final retreat of the Paratethys Sea) (Figure 1.5).

Precipitation strengthens over southern Asia (Figure 1.5), especially over the Himalayan range (Sarr et al. 2022) and eastern China (Farnsworth et al. 2019).

However, summer winds in the Arabian Sea region are still too weak to trigger ocean upwelling. The increase in land exposure in the Arabian Peninsula region combined with the uplift of the East African highlands (Africa), Zagros range and Anatolian Plateau (Middle-East) allow us to strengthen the Somali Jet and promote the development of oceanic upwelling in the Arabian Sea during the Late Miocene (Figure 1.6, Sarr et al. 2022).

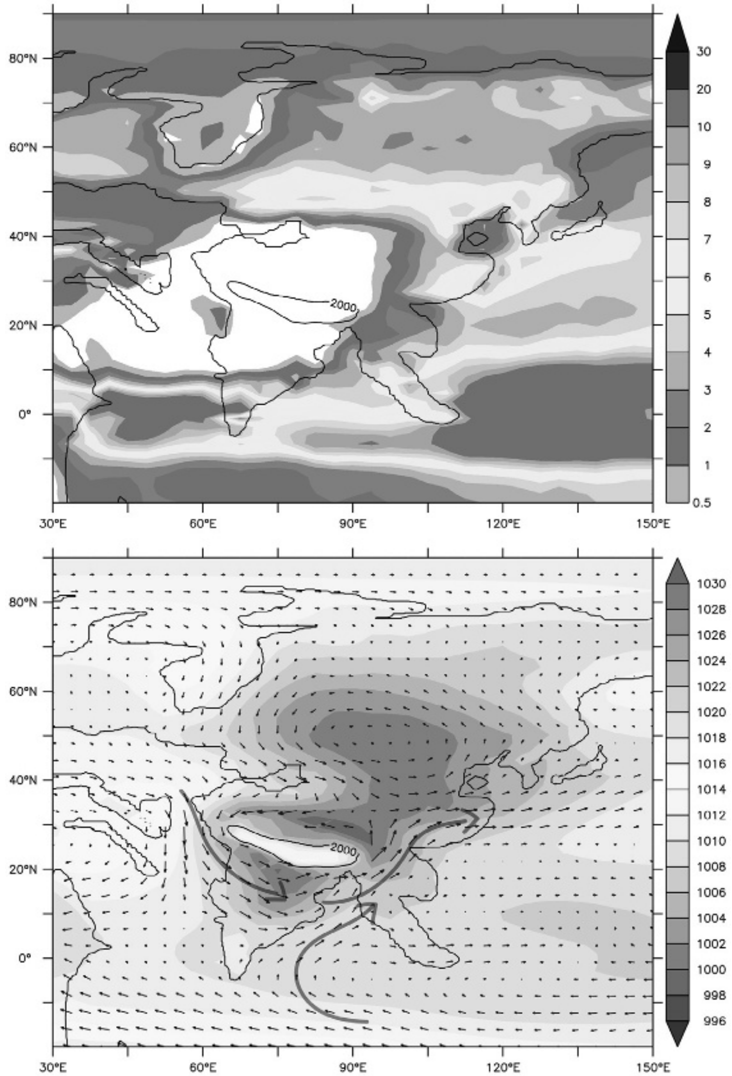

Figure 1.4. *Late Eocene (40Ma) simulated climate with the ESM IPSL-CM5A2. Upper: mean summer precipitation (top – in mm/day). Lower: mean sea level pressure (shading – in hPa) and 850 hPa wind (vectors) in summer. Topography contoured at 2,000 m (4,000 m) in a thin solid (dash) line. The pCO_2 is fixed at 1,160 ppmv. For a color version of this figure, see www.iste.co.uk/cattin/himalaya3.zip*

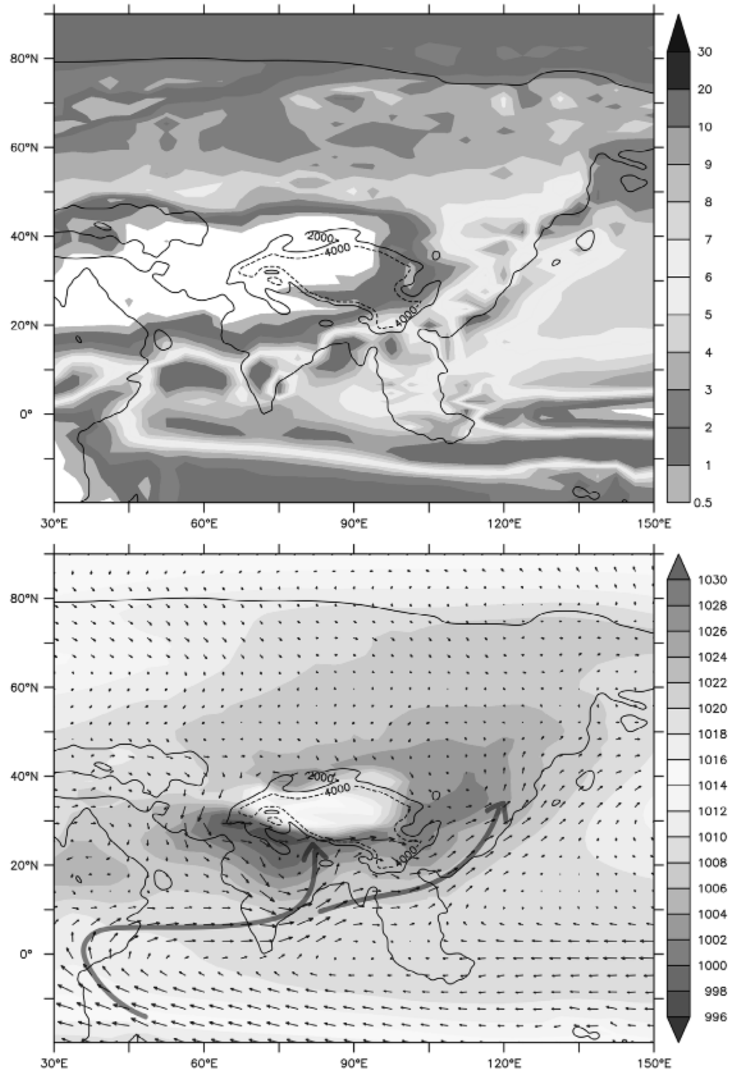

Figure 1.5. *Early Miocene (20 Ma) simulated climate with the ESM IPSL-CM5A2. Same as Figure 1.4. The pCO_2 is fixed at 560 ppmv. For a color version of this figure, see www.iste.co.uk/cattin/himalaya3.zip*

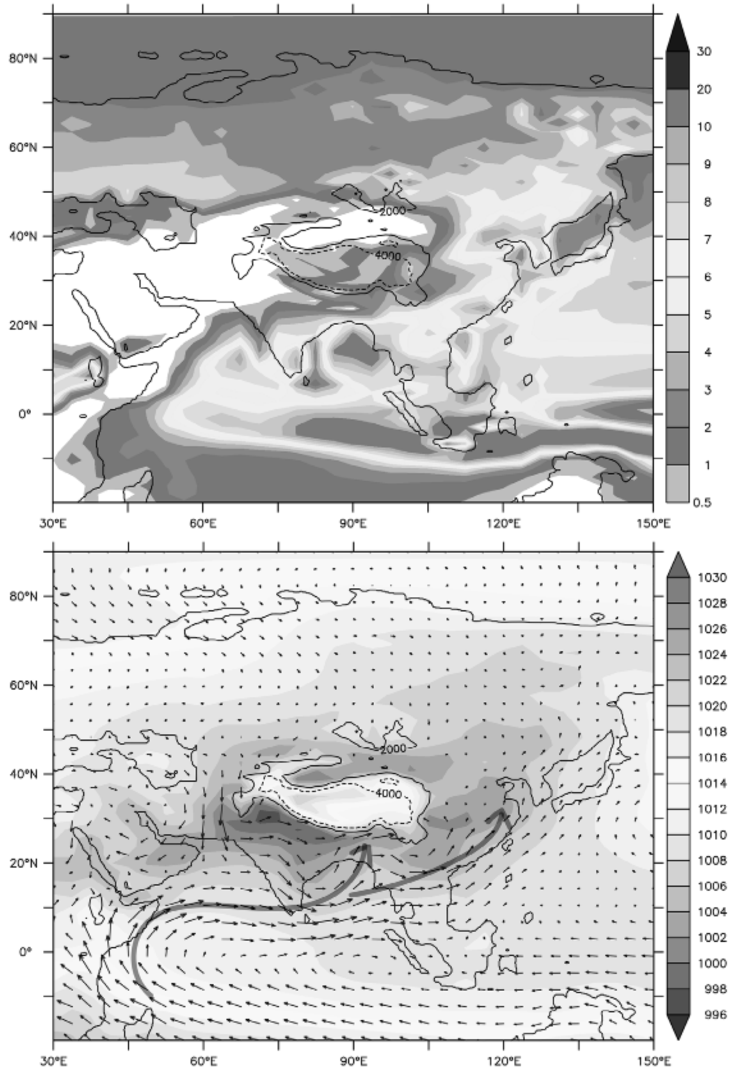

Figure 1.6. *Late Miocene (11 Ma) simulated climate with the ESM IPSL-CM5A2. Same as Figure 1.4. The pCO_2 is fixed at 420 ppmv. For a color version of this figure, see www.iste.co.uk/cattin/himalaya3.zip*

1.4.2. *Impact of orogenesis on the ocean circulation*

Earth System Models also help us to quantify the effects of orogenesis on the ocean circulation. Yang and Wen (2020) showed that when Asian reliefs are removed on a present-day geography, the intensity of the Atlantic meridional overturning circulation (AMOC) is reduced by about 80% in response to the enhancement of the buoyancy of surface waters in the Norwegian Sea. Changes in mid-latitude westerly winds and weakening trade winds over the Pacific Ocean result in the cooling of surface waters in the North Atlantic and a transfer of freshwater (through changes in the hydrological cycle) from the Pacific region to the Atlantic, which results in a decrease of surface water salinity in the North Atlantic. Assuming a nearly flat Earth (<200 m), Maffre et al. (2018) showed that deep water formation shifts from the Norwegian Sea (Atlantic Ocean) to the Gulf of Alaska (Pacific Ocean).

Removing topography has consequences on the surface temperature due to the changes in the atmospheric circulation. The mean annual temperature anomalies (flat Earth experiment minus present-day Earth experiment) corrected by a vertical temperature gradient of 6.14°C/km highlight the region where the warming–cooling patterns are related to dynamical changes (in other words, deviate from adiabatic cooling). The removal of Rockies causes the cooling (warming) of western (eastern) North America (Figure 1.7). The same phenomenon occurs in Asia with a cooling west of Tibet and a warming on the east coast. The decrease of surface temperature exceeds 4°C in the North Atlantic Ocean and 8°C in the Norwegian sea.

The warming–cooling patterns are clearly related to changes in the large-scale Rossby waves which are almost zonal in the case of flat Earth (Figure 1.8). The lack of topography also favors a transfer of freshwater from the Indian Ocean to the Atlantic Ocean (via the African continent) with a consequent decrease in surface water salinity in the central Atlantic Ocean (Figure 1.7). In the mid-latitudes, the removal of the North American Cordillera induces the transfer of freshwater from the Pacific Ocean to the Atlantic Ocean. This results in an increase (decrease) of the surface salinity in the North Pacific (North Atlantic) Ocean (Figure 1.7). Isotopic measurements ($\delta^{18}O$ and $\delta^{13}C$) on benthic foraminifera from the Atlantic Ocean suggest the establishment of the AMOC around the Eocene–Oligocene boundary

(Hutchinson et al. 2021). In addition to the effect of orogenesis, the ocean circulation is obviously influenced by the closure or opening of ocean gateways during the Cenozoic (Drake, Tasman Sea, Greenland–Scotland Ridge, Fram, etc.).

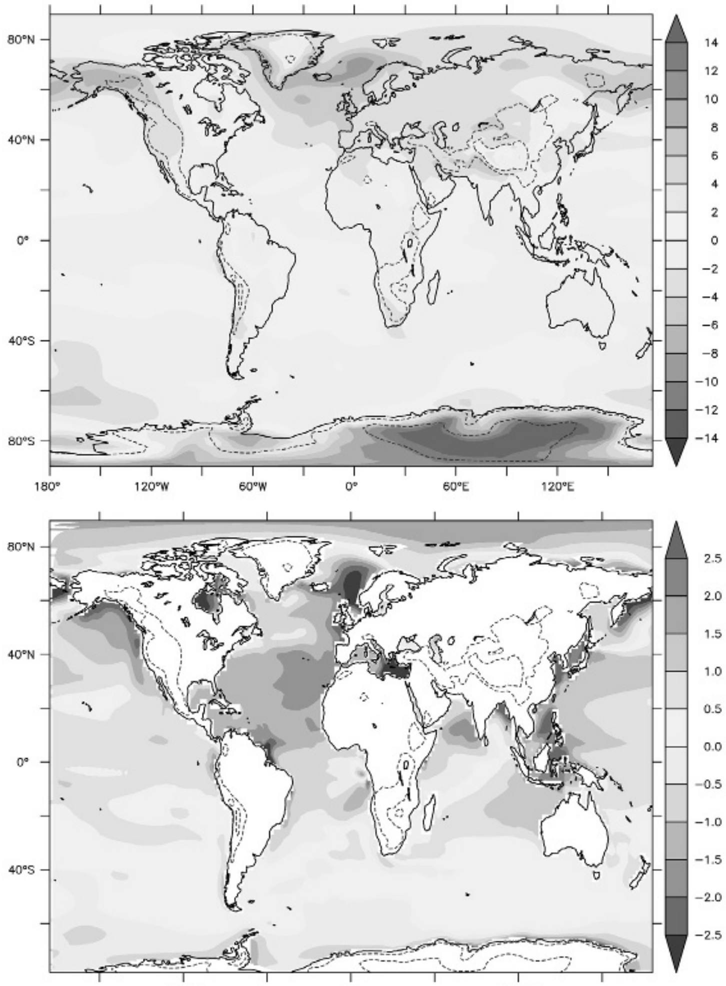

Figure 1.7. *Upper: shaded anomaly (flat Earth minus present-day Earth) of air temperature at 2 m (in °C), annual mean, corrected by a 6.14°C/km lapse rate (after (Maffre et al. 2018)). Lower: shaded anomaly (flat Earth minus present-day Earth) of salt in surface ocean (in psu), annual mean. For a color version of this figure, see www.iste.co.uk/cattin/himalaya3.zip*

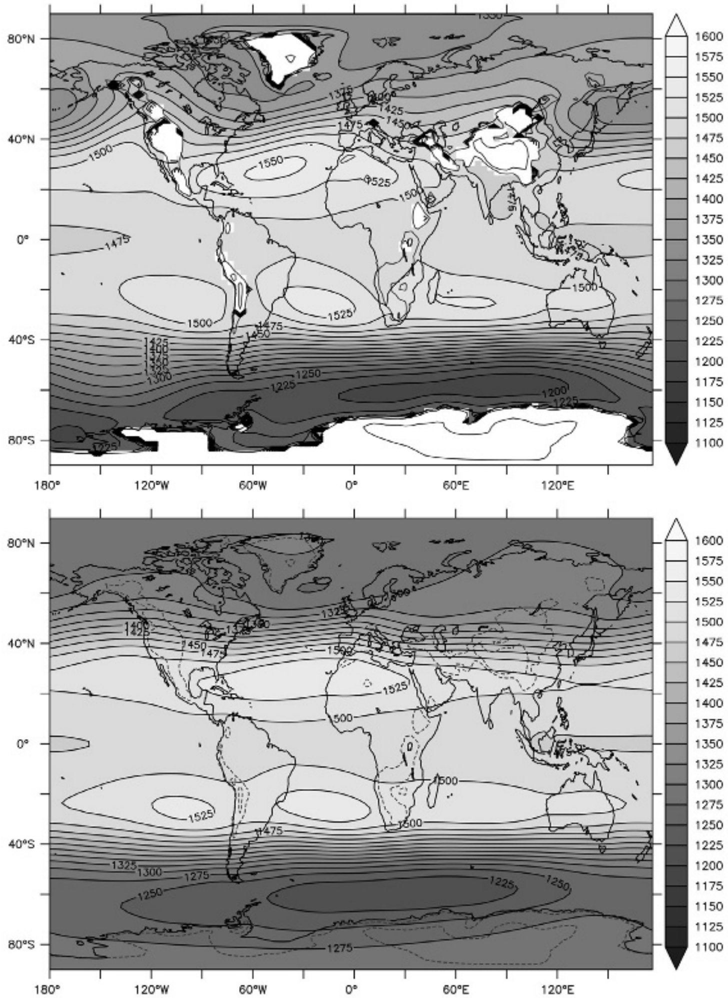

Figure 1.8. *Upper: shaded geopotential height at 850 hPa (m) for present-day simulation, annual mean. Lower: same for the flat Earth experiment (after (Maffre et al. 2018)). For a color version of this figure, see www.iste.co.uk/cattin/himalaya3.zip*

1.4.3. *Impact of orogenesis on the chemical composition of the atmosphere*

In 1899, Chamberlin (1899) suggested in a pioneering work that chemical weathering of silicates associated with mountain uplifts controls climate at a geological timescale. Ninety years later, Raymo et al. (1988) based on ocean records such as the $^{87}Sr/^{86}Sr$ ratio of the ocean concluded that the Himalayan and Tibetan uplifts during the Cenozoic increased physical erosion and enhanced the chemical weathering of sediments with a consequent decrease in the atmospheric CO_2 concentration (pCO_2) and global cooling. While these landforms are all driven by mantle dynamics, their evolution is the result of both endogenous (tectonics) and exogenous (erosion) processes (Champagnac et al. 2012). The erosion rate of a mountain range varies with tectonic activity and climatic context (precipitation and temperature). Fission tracks on apatite collected from the Bay of Bengal sediments trace the exhumation of Himalayan range rocks. However, this rate, estimated at 1–3 km/Ma for the past 13 Ma, appears to be relatively insensitive to climate variations (Huyghe et al. 2020).

Orogenesis obviously has a crucial role as ~40% of chemical weathering is estimated to occur on ~10% of the steepest continental surfaces (Larsen et al. 2014). Yet, carbon consumption by dissolved elements from the Himalayan range (~0.19×10^{12} molC/yr) is only 6% of the total annual flux (3.2×10^{12} molC/yr). The low silicate weathering can be related to a too fast transfer of sediments to the ocean compared to the reaction kinetics of mineral alteration, and the lithology of Himalayan rocks would not be the most favorable (reduced amount of calcium silicate). The consumption of carbon in an orogenic context can take other forms. The transfer and burial of continental organic matter in sedimentary basins has been a very effective mechanism (France-Lanord and Derry 1997). Finally, the orogenic context can be a source of carbon through the oxidation of exhumed organic-rich rocks or sulfide minerals such as pyrite (Hilton and West 2020).

1.5. Conclusion

Climate changes in Asia are largely attributable to paleogeographic changes. The uplifts of the Himalayan range, Tibetan plateau or more modest landforms indeed strongly modify the atmospheric circulation. Associated with other paleogeographic changes (such as the retreat of an epicontinental sea, the uplift of landforms out of Asia or the increase in land exposure in the Arabian Peninsula), the distribution of precipitation has changed spatially and seasonally during the Cenozoic. The uplift of the Himalaya and adjacent landforms (Zagros, Karakorum) progressively reduces the exchanges between mid- and low latitudes and favors the onset of a modern monsoon regime in Asia from the early Miocene, while the uplift of the Tibetan plateau (especially its northern part) disrupts the western moisture flow leading to aridification of Central Asia and to an increase in precipitation in eastern China during spring and summer.

Orogenies cause disturbances in the global ocean by acting on the atmospheric circulation and heat exchanges. One of the consequences of the Cenozoic orogenies is the shift of deep water formation from the Pacific Ocean to the Atlantic Ocean. The response of the ocean is much more complex because the geometry of the basins has also changed.

Finally, the uplift of the landforms in Asia indirectly disrupts the climate by affecting the sources (oxidation) and sinks (chemical alteration and burial of organic matter) of carbon.

Can these mechanisms be transposed to other orogenies? The impact of orogeny on climate depends on the characteristics of the range (horizontal and vertical extensions) and the climatic context. Let us take the example of the Andes in South America. This range deflects the trade winds coming from the equatorial Atlantic Ocean into a powerful northerly flow (South American Low-Level Jet) transporting moisture from the Amazon basin to the subtropics and the Andean piedmont. This results in significant orographic precipitation in summer on the eastern flank of the Andes up to 30°S. Insel et al. (2010) shows with a regional climate model that reducing the Andean range elevation to half the present day induces a strong attenuation of the South American Low-Level Jet and suppression of moisture transport to the Andean foothills, resulting in an increase in precipitation over the Amazon basin. These results are in agreement with different paleoclimatic indicators (fauna, flora) that show an increase in precipitation around 10 Ma on the eastern flank of the Andes. The increase in precipitation is reflected by an acceleration of the exhumation rates inferred from fission tracks on apatite in the Central Andean thrust belt (Barnes et al. 2012). On the Pacific side, the semi-arid climate is replaced by a hyper-arid climate, ending supergene weathering (Strecker et al. 2007).

The impact of orogenies on climate has undoubtedly evolved since the earliest ages of the Earth as landforms have changed. In the late Archaean, high crustal and mantle radiogenic heat production as well as numerous magmatic intrusions within the early cratons limit the lithosphere's strength to support high topography (Rey and Houseman 2006). Rey and Coltice (2008) estimates that landforms should not have exceeded 1,800–2,000 m assuming a modern deformation rate (10^{-15}–10^{-14} s^{-1}). During the Proterozoic, secular cooling of the Earth favors a thicker and more rigid lithosphere favoring deformations at the boundaries of cratons. The orogenies at that time do not yet have the characteristics of modern orogenies, which could mean lower elevation than today. Ultra-high-pressure metamorphism (notably the blue shale facies) which is frequently found in the collision chains (see Volume 2 – Chapter 4) and is synonymous of modern-type orogenies, only dates back from the Neoproterozoic (approximately 600–800 Ma ago).

1.6. References

Acosta, R.P. and Huber, M. (2020). Competing topographic mechanisms for the summer Indo-Asian Monsoon. *Geophys Res Lett*, 47(3), e2019GL085112.

Barbolini, N., Woutersen, A., Dupont-Nivet, G., Silvestro, D., Tardif, D., Coster, P.M.C., Meijer, N., Chang, C., Zhang, H.X., Licht, A. et al. (2020). Cenozoic evolution of the steppe-desert biome in Central Asia. *Sci Adv*, 6(41), eabb8227.

Barnes, J.B., Ehlers, T.A., Insel, N., McQuarrie, N., Poulsen, C.J. (2012). Linking orography, climate, and exhumation across the central Andes. *Geology*, 40(12), 1135–1138.

Bhatia, H., Srivastava, G., Spicer, R.A., Farnsworth, A., Spicer, T.E.V., Mehrotra, R.C., Spicer, T.E.V., Bera, S., Valdes, P. (2021). Leaf physiognomy records the Miocene intensification of the South Asia Monsoon. *Glob Planet Change*, 196, 103365.

Bolin, B. (1950). On the influence of the Earth's orography on the general character of the Westerlies. *Tellus*, 2(3), 184–195.

Boos, W.R. and Kuang, Z. (2010). Dominant control of the South Asian monsoon by orographic insulation versus plateau heating. *Nature*, 463(7278), 218–222.

Botsyun, S., Sepulchre, P., Donnadieu, Y., Risi, C., Licht, A., Caves Rugenstein, J.K. (2019). Revised paleoaltimetry data show low Tibetan Plateau elevation during the Eocene. *Science*, 363(6430), eaaq1436.

Chamberlin, T.C. (1899). An attempt to frame a working hypothesis of the cause of glacial periods on an atmospheric basis. *J Geol*, 7(6), 545–584.

Champagnac, J.-D., Molnar, P., Sue, C., Herman, F. (2012). Tectonics, climate, and mountain topography. *J Geophys Res Solid Earth*, 117, B02403.

Charney, J. and Eliassen, A. (1949). A numerical method for predicting the perturbations of the middle latitude westerlies. *Tellus*, I(2), 38–54.

Clift, P.D. and Webb, A.A.G. (2019). History of the Asian monsoon and its interactions with solid earth tectonics in Cenozoic South Asia. *Geol Soc Lond Spec Publ*, 483, 875–880.

Dettman, D.L., Kohn, M.J., Quade, J., Ryerson, F.J., Ojha, T.P., Hamidullah, S. (2001). Seasonal stable isotope evidence for a strong Asian monsoon throughout the past 10.7 my (2001). *Geology*, 29, 31–34.

Ding, Y. and Krishnamurti, T. (1987). Heat budget of the Siberian High and the winter monsoon. *Mon Weather Rev*, 115, 2428–2449.

Ding, L., Spicer, R., Yang, J., Xu, Q., Cai, F., Li, S., Lai, Q.,Wang, H., Spicer, T., Yue, Y. et al. (2017). Quantifying the rise of the Himalaya orogen and implications for the South Asian monsoon. *Geology*, 45(3), 215–218.

Fang, X., Zan, J., Appel, E., Lu, Y., Song, C., Dai, S., Tuo, S. (2015). An Eocene–Miocene continuous rock magnetic record from the sediments in the Xining Basin, NW China: Indication for Cenozoic persistent drying driven by global cooling and Tibetan Plateau uplift. *Geophys J Int*, 201(1), 78–89.

Fang, X., Yan, M., Zhang, W., Nie, J., Han, W., Wu, F., Song, C., Zhang, T., Zan, J., Yang, Y. (2021). Paleogeography control of Indian monsoon intensification and expansion at 41 Ma. *Sci Bull*, 66(22), 2320–2328.

Farnsworth, A., Lunt, D.J., O'Brien, C.L., Foster, G.L., Inglis, G.N., Markwick, P., Pancost, R.D., Robinson, S.A. (2019). Climate sensitivity on geological timescales controlled by nonlinear feedbacks and ocean circulation. *Geophy Res Lett*, 46(16), 9880–9889.

Fluteau, F., Ramstein, G., Besse, J. (1999). Simulating the evolution of the Asian and African monsoons during the past 30Myr using an atmospheric general circulation model. *J Geophys Res Atmos*, 104(D10), 11995–12018.

France-Lanord, C. and Derry, L.A. (1997). Organic carbon burial forcing of the carbon cycle from Himalayan erosion. *Nature*, 390(6655), 65–67.

Gebelin, A., Mulch, A., Teyssier, C., Jessup, M.J., Law, R.D., Brunel, M. (2013). The Miocene elevation of Mount Everest. *Geology*, 41(7), 799–802.

Guo, Z.T., Sun, B., Zhang, Z.S., Peng, S.Z., Xiao, G.Q., Ge, J.Y., Hao, Q.Z., Qiao, Y.S., Liang, M.Y., Liu, J.F. et al. (2008). A major reorganization of Asian climate by the early Miocene. *Clim Past*, 4(3), 153–174.

Gupta, A.K., Yuvaraja, A., Prakasam, M., Clemens, S.C., Velu, A. (2015). Evolution of the South Asian monsoon wind system since the late Middle Miocene. *Palaeogeogr Palaeoclimatol Palaeoecol*, 438, 160–167.

Hahn, D.G. and Manabe, S. (1975). The role of mountains in the South Asian monsoon circulation. *J Atmos Sci*, 32, 1515–1541.

Halley, E. (1686). An historical account of the trade winds and monsoons observable in the seas between and near the tropics with an attempt to assign a physical cause of the said winds. *Philos Trans R Soc London*, 16, 153–168.

Hersbach, H., Bell, B., Berrisford, P., Biavati, G., Horanyi, A., Munõz Sabater, J., Nicolas, J., Peubey, C., Radu, R., Rozum, I. et al. (2019). ERA5 monthly averaged data on single levels from 1979 to present. Copernicus Climate Change Service (C3S) Climate Data Store (CDS). 10.24381/cds.f17050d7 [Online]. Available at: https://www.ecmwf.int/en/ forecasts/dataset/ecmwf-reanalysis-v5 [Accessed 15 March 2022].

Hilton, R.G. and West, A.J. (2020). Mountains, erosion and the carbon cycle. *Nat Rev Earth Environ*, 1(6), 284–299.

Hutchinson, D.K., Coxall, H.K., Lunt, D.J., Steinthorsdottir, M., de Boer, A.M., Baatsen, M., von der Heydt, A., Huber, M., Kennedy-Asser, A.T., Kunzmann, L. et al. (2021). The Eocene-Oligocene transition: A review of marine and terrestrial proxy data, models and model-data comparisons. *Clim Past*, 17, 269–315.

Huyghe, P., Bernet, M., Galy, A., Naylor, M., Cruz, J., Gyawali, B.R., Gemignani, L., Mugnier, J.L. (2020). Rapid exhumation since at least 13 Ma in the Himalaya recorded by detrital apatite fission-track dating of Bengal fan (IODP Expedition 354) and modern Himalayan river sediments. *Earth and Planet Sci Lett*, 534, 116078.

Insel, N., Poulsen, C.J., Ehlers, T.A. (2010). Influence of the Andes Mountains on South American moisture transport, convection, and precipitation. *Clim Dyn*, 35, 1477–1492.

Kutzbach, J.E., Guetter, P.L., Ruddiman, W.F., Prell, W.L. (1989). Sensitivity of climate to Late Cenozoic uplift in Southern Asia and the American West: Numerical experiments. *J Geophys Res*, 94, 18393–18407.

Ladant, J.-B., Donnadieu, Y., Dumas, C. (2014). Links between CO2, glaciation and water flow: Reconciling the Cenozoic history of the Antarctic Circumpolar Current. *Clim Past*, 10(6), 1957–1966.

Larsen, I.J., Montgomery, D.R., Greenberg, H.M. (2014). The contribution of mountains to global denudation. *Geology*, 42(6), 527–530.

Licht, A., van Cappelle, M., Abels, H.A., Ladant, J.-B., Trabucho-Alexandre, J., France-Lanord, C., Donnadieu, Y., Vandenberghe, J., Rigaudier, T., Lécuyer, C. et al. (2014). Asian monsoons in a late Eocene greenhouse world. *Nature*, 513(7519), 501–506.

Maffre, P., Ladant, J.B., Donnadieu, Y., Sepulchre, P., Goddéris, Y. (2018). The influence of orography on modern ocean circulation. *Clim. Dyn*, 50, 1277–1289.

Manabe, S. and Terpstra, T.B. (1974). The effects of mountains on the general circulation of the atmosphere as identified by numerical experiments, *J Atmos Sci*, 31, 3–42.

McGuffie, K. and Henderson-Sellers, A. (2005). *A Climate Modelling Primer*, 3rd edition. John Wiley & Sons, Chichester, West Sussex; Hoboken, NJ.

Meijer, N., Dupont-Nivet, G., Abels, H.A., Kaya, M.Y., Licht, A., Xiao, M.M., Zhang, Y., Roperch, P., Poujol, M., Lai, Z.P. et al. (2019). Central Asian moisture modulated by proto-Paratethys Sea incursions since the early Eocene. *Earth Planet Sci Lett*, 510, 73–84.

Mintz, Y. (1965). Very long-term global integration of the primitive equations of atmospheric motion. *WMO Tech Note*, 66, 141–167.

Mulch, A. (2016). Stable isotope paleoaltimetry and the evolution of landscapes and life. *Earth Planet Sci Lett*, 433, 180–191

Quade, J., Cerling, T.E., Bowman, J.R. (1989). Development of Asian monsoon revealed by marked ecological shift during the latest Miocene in Northern Pakistan. *Nature*, 342, 163–166.

Rey, P.F. and Coltice, N. (2008). Neoarchean strengthening of the lithosphere and the coupling of the Earth's geochemical reservoirs. *Geology*, 36, 635–638.

Rey, P.F. and Houseman, G. (2006). Lithospheric scale gravitational flow: The impact of body forces on orogenic processes from Archaean to Phanerozoic. *Geol Soc Lond Spec Pub*, 253(1), 153–167.

Rowley, D.B. and Garzione, C.N. (2007). Stable isotope-based paleoaltimetry. *Annu Rev Earth Planet Sci*, 35, 463–508.

Ruddiman, W.F. and Kutzbach, J.E. (1989). Forcing of late Cenozoic northern hemisphere climate by plateau uplift in southern Asia and the American west. *J Geophys Res*, 94, 18409–18427.

Sarr, A.C., Donnadieu, Y., Bolton, C.T., Ladant, J.B., Licht, A., Fluteau, F., Laugié, M., Tardif, D., Dupont-Nivet, G. (2022). Neogene South Asian monsoon rainfall and wind histories diverged due to topographic effects. *Nat Geosci*, 15, 314–319.

Sepulchre, P., Caubel, A., Ladant, J.-B., Bopp, L., Boucher, O., Braconnot, P., Brockmann, P., Cozic, A., Donnadieu, Y., Dufresne, J.-L. et al. (2020). IPSL-CM5A2 – An Earth system model designed for multi-millennial climate simulations. *Geosci Model Dev*, 13(7), 3011–3053.

Sorrel, P., Eymard, I., Leloup, P.-H., Maheo, G., Olivier, N., Sterb, M., Gourbet, L., Wang, G., Jing, W., Lu, H. et al. (2017). Wet tropical climate in SE Tibet during the Late Eocene. *Sci Rep*, 7(1), 1–11.

Spicer, R.A., Yang, J., Herman, A., Kodrul, T., Aleksandrova, G., Maslova, N., Spicer, T., Ding, L., Xu, Q., Shukla, A. et al. (2017). Paleogene monsoons across India and South China: Drivers of biotic change. *Gondwana Res*, 49, 350–363.

Spicer, R.A., Hoorn, C., Perrigo, A., Antonelli, A. (2018). Phytopaleoaltimetry: Using plant fossils to measure past land surface elevation. In *Mountains, Climate and Biodiversity*, Hoorn, C., Perrigo, A., Antonelli, A. (ed.). Wiley, Oxford.

Strecker, M.R., Alonso, R.N., Bookhagen, B., Carrapa, B., Hilley, G.E., Sobel, E.R., Trauth, M.H. (2007). Tectonics and climate of the southern Central Andes. *Ann Rev Earth Planet Sci*, 35, 747–787.

Su, T., Spicer, R.A., Wu, F.X., Farnsworth, A., Huang, J., Rio, C.D., Deng, T., Ding, L., Deng, W.Y.D., Huang, Y.J. et al. (2020). A Middle Eocene lowland humid subtropical "Shangri-La" ecosystem in central Tibet. *PNAS*, 117(52), 32989–32995.

Sun, X. and Wang, P. (2005). How old is the Asian monsoon system? Palaeobotanical records from China. *Palaeogeogr Palaeoclimatol Palaeoecol*, 222(3–4), 181–222.

Tardif, D., Fluteau, F., Donnadieu, Y., Le Hir, G., Ladant, J.-B., Sepulchre, P., Licht, A., Poblete, F., Dupont-Nivet, G. (2020). The origin of Asian monsoons: A modelling perspective. *Clim Past*, 16(3), 847–865.

Tauxe, L. and Feakins, S.J. (2020). A reassessment of the chronostratigraphy of Late Miocene C3–C4 transitions. *Paleoceanogr Paleoclimatol*, 35, e2020PA003857.

Webster, P.J., Magana, V.O., Palmer, T.N., Shukla, J., Tomas, R.A., Yanai, M., Yasuna, T. (1998). Monsoons: Processes, predictability, and the prospects for prediction. *J Geophys Res*, 103(C7), 14451–14510.

Westerhold, T., Marwan, N., Drury, A.J., Liebrand, D., Agnini, C., Anagnostou, E., Barnet, J.S.K., Bohaty, S.M., De Vleeschouwer, D., Florindo, F. et al. (2020). An astronomically dated record of Earth's climate and its predictability over the last 66 million years. *Science*, 369(6509), 1383–1387.

Yang, H. and Wen, Q. (2020). Investigating the role of the Tibetan plateau in the formation of Atlantic Meridional Overturning Circulation. *J Clim*, 33(9), 3585–3601.

Zhao, L., Lu, H.Y., Wang, H.L., Meadows, M., Ma, C.M., Tang, L.Y., Lei, F., Zhang, H.Y. (2020). Vegetation dynamics in response to evolution of the Asian Monsoon in a warm world: Pollen evidence from the Weihe Basin, central China. *Glob Planet Change*, 193, 103269.

Zoura, D., Hill, D., Dolan, A., Hunter, S., Tang, Z., Haywood, A. (2019). Atmospheric carbon dioxide, ice sheet and topographic constraints on palaeo moisture availability in Asia. *Earth Planet Sci Lett*, 519, 12–27.